Submitted to the International Europhysics Conference on High Energy Physics,
HEP97, Jerusalem, Israel, August 1997

Leading Neutron Production in Deep Inelastic Scattering at HERA

H1 Collaboration

Abstract

Events with a high energy neutron produced at a small angle with respect to the proton beam direction have been observed by the H1 experiment at HERA. The observed energy and $|t|$ distributions of final-state neutrons are compared with the predictions of Monte Carlo models based upon pion exchange and soft color interactions. Both models are in general agreement with the data for events containing a neutron with energy $E_n \geq 400$ GeV. In the kinematic range $5 \leq Q^2 \leq 100$ GeV^2 and $0.05 \leq y \leq 0.7$, the fraction of DIS events containing a leading neutron with $E_n \geq 400$ GeV and $|t| \leq 0.5$ GeV^2 is $(7.8^{+3.0}_{-2.0})\%$. The differential cross section $\mathrm{d}\sigma(ep \to e'nX)/\mathrm{d}z$ has been measured for $z \geq 0.4$ and $|t| \leq 0.5$ GeV^2, where z is the fraction of the incident proton's momentum carried by the final-state neutron.

Abstract 378
Parallel Sessions 2,3,4
Plenary Sessions 1,2,3

Introduction

The H1 experiment used a new forward neutron calorimeter (FNC) during 1996 to obtain $ep \to e'nX$ data [1]. Semi-inclusive neutron production in deep inelastic scattering (DIS) is of theoretical interest because virtual pion exchange is expected to be the dominant production mechanism at large z and small momentum transfers with $|t| \ll 1$ GeV^2 [2, 3, 4, 5]. An alternative mechanism, where neutrons are predominantly produced as a result of soft color interactions and the hadronization of the proton remnant is also possible [6]. In this paper, we compare our leading neutron data with two different Monte Carlo models, in order to test these alternative production mechanisms. In addition, we report on our measurement of $\mathrm{d}\sigma(ep \to e'nX)/\mathrm{d}z$.

In order to completely specify the kinematics of the $ep \to e'nX$ process shown in Fig. 1, four Lorentz scalars are needed

$$\begin{array}{ll} Q^2 = -(k-k')^2 & y = 2p\cdot(k-k')/s \\ t = (p-p')^2 & z = 1 - 2k\cdot(p-p')/s. \end{array} \tag{1}$$

These Lorentz invariants give the lepton and baryon currents a symmetric treatment. Throughout this paper we make the approximation $z = E_n/E_p$ where E_n and E_p are the energies of the final-state neutron and incident proton beam respectively. The four-momentum of the final-state neutron p' is calculated using the neutron's energy and impact position at the forward neutron calorimeter. These quantities, along with measurement of the main interaction vertex in the H1 central detector, allows p' to be completely determined.

The one-photon exchange cross section for deep inelastic scattering defines the proton structure function $F_2^p(x, Q^2)$

$$\frac{\mathrm{d}\sigma(ep \to e'X)}{\mathrm{d}x\,\mathrm{d}Q^2} = \frac{2\pi\alpha^2}{Q^4 x}\,[2 - 2y + \frac{y^2}{1+R}]\,F_2^p(x, Q^2), \tag{2}$$

where α is the fine structure constant and $R = F_2^p(x, Q^2)/2xF_1^p(x, Q^2) - 1$. According to models of pion exchange, the cross section for semi-inclusive neutron production is given by an analogous equation

$$\frac{\mathrm{d}\sigma(ep \to e'nX)}{\mathrm{d}x\,\mathrm{d}Q^2\,\mathrm{d}z\,\mathrm{d}t} = f_{n/p}(z,t)\,\frac{2\pi\alpha^2}{Q^4 x}\,[2 - 2y + \frac{y^2}{1+R}]\,F_2^\pi(\beta, Q^2), \tag{3}$$

where $F_2^\pi(\beta, Q^2)$ is the structure function of the pion. The Bjorken variable in the electron – pion deep inelastic scattering is $\beta = x/(1-z)$. The flux of neutrons inside the proton $f_{n/p}(z,t)$ can be parameterized as [4, 7]

$$f_{n/p}(z,t) = \frac{2g^2_{p\pi^0 p}}{16\pi^2}\,(1-z)\,\frac{-t}{(m_\pi^2 - t)^2}\,\exp\left\{-\frac{m_\pi^2 - t}{\Lambda^2\,(1-z)}\right\}, \tag{4}$$

where m_π is the mass of the pion and $g^2_{p\pi^0 p}/4\pi = (13.6 \pm 0.8)$ and $\Lambda = (1.1 \pm 0.1)$ GeV are parameters determined by previous experiments [8, 9, 10, 11, 12, 13, 14, 15].

The POMPYT 2.6 Monte Carlo program [7] uses Equations 3 and 4 to model meson exchange. The final-state neutron is a spectator in the $\gamma^* - \pi^+$ deep inelastic scattering reaction. The independence of the neutron flux factor $f_{n/p}(z,t)$ and the pion structure function $F_2^\pi(\beta, Q^2)$, what is referred to as factorization, is a theoretical assumption which we plan to test in the future. The POMPYT Monte Carlo program has been used previously to investigate the characteristics of pion exchange at HERA [16].

LEPTO 6.5 [6] is a Monte Carlo program which uses soft color interactions and an implementation of the string fragmentation model [17] to produce final-state neutrons. Soft color interactions were originally introduced into the LEPTO 6.5 Monte Carlo model in order to explain the observation of large rapidity gap events at HERA. Recently soft color interactions have also been used to explain the excess of charm and beauty production at the Tevatron [18]. The neutron energy spectrum predicted by the LEPTO 6.5 Monte Carlo model is harder than the distribution predicted by earlier versions of this program. After the exchange of a soft gluon, the proton remnant may become a color singlet and fragment independently of the hard scattering system. If a soft gluon had not been exchanged, there would be a string connecting the hard scattering system and the proton remnant. The presence of a string between the two systems would result in lower energy for the final-state baryon produced during the fragmentation process.

Event Selection

The selection criteria $5 \leq Q^2 \leq 100$ GeV^2 and $0.05 < y < 0.7$ have been applied to the data presented in this paper. The kinematic quantities Q^2 and y were determined using the electron method which only requires determination of the four-momentum of the scattered positron. The main vertex was required to be in the region $-25 \leq z_{\rm vtx} \leq 35$ cm and the energy of the scattered positron E' was required to be $E' \geq 8$ GeV. DIS events containing a high energy neutron were triggered by requiring an energy deposit in the new backward electromagnetic calorimeter (Spacal) in coincidence with a cluster in the forward neutron calorimeter. The data presented in this paper corresponds to an integrated luminosity of 1.98 pb^{-1} which is approximately 25% of the total 1996 data sample.

Description of the Forward Neutron Calorimeter

The H1 forward neutron calorimeter is situated in the HERA tunnel at a distance of 107 m away from the nominal interaction region. A schematic diagram of the FNC is shown in Fig. 2. It is a modified version of the SPACAL calorimeter developed by the LAA project at CERN [19, 20]. The calorimeter consists of interleaved layers of lead and 2 m long scintillating fibers. The calorimeter is 9.5 nuclear interaction-lengths deep ($\lambda_I \approx 21$ cm) and is laterally segmented into 75 hexagonal towers. Each tower is defined by coupling 1141 scintillating fibers to a common photomultiplier located at the rear of the detector. Two segmented planes of hodoscopes situated in front of the FNC are used to veto charged particles. A detailed view of the lead/scintillating fiber matrix used to construct the calorimeter modules is shown in Fig. 3.

Comparison with Monte Carlo Models

Fig. 4 shows that at the generator level, without any detector resolution or acceptance effects, the LEPTO and POMPYT Monte Carlo programs give very different predictions for the shape of the neutron energy spectra. The dashed curves show the predictions for the energy spectra after the FNC acceptance has been taken into account. The observed neutron energy distribution is not a significant test of the different production models because of the influence of the FNC acceptance.

The absolute normalization of the Monte Carlo predictions shown in Fig. 4 depend upon the values of the structure functions used in the calculations. The CTEQ2L parton distributions for the proton [21] were used to calculate the LEPTO Monte Carlo predictions. The absolute normalization of the POMPYT Monte Carlo prediction has large uncertainty because it depends upon the value of the pion structure function which has not been measured for $x \leq 0.1$. If one uses the Glück, Reya, and Vogt (GRV) leading order parton distributions for the pion [22], both Monte Carlo programs result in predictions that have approximately the same order of magnitude in the high energy region with $600 \leq E_n \leq 800$ GeV.

Fig. 5 shows the observed neutron energy and $|t|$ distributions for DIS events containing a high energy neutron. The solid points are data and the histograms show the predictions of the LEPTO and POMPYT Monte Carlo programs after simulating the FNC acceptance and energy resolution. The LEPTO Monte Carlo predictions are normalized to the number of events observed in the data with $E_n \geq 100$ GeV, whereas the POMPYT Monte Carlo predictions, shown in Figures 5A and 5C, are normalized to the number of events observed in the data with $E_n \geq 400$ GeV. A Gaussian neutron energy resolution of 25% is used in these simulations which gives a good description of the high energy tail present in the data. Both Monte Carlo programs are in general agreement with the data for events with a neutron with energy $E_n \geq 400$ GeV and $|t| \leq 1$ GeV^2.

Fig. 6 shows the observed neutron p_T distributions in different energy ranges compared to the predictions of the LEPTO and POMPYT Monte Carlo models after simulating the FNC acceptance and energy resolution. The transverse momentum p_T is calculated with respect to the incident proton beam direction. The LEPTO Monte Carlo predictions are normalized to the number of events observed in the data with $E_n \geq 100$ GeV. The POMPYT Monte Carlo predictions are normalized to the number of events observed in the data with $E_n \geq 400$ GeV and are only shown in this kinematic region. There is general agreement between the data and the LEPTO Monte Carlo predictions in all energy ranges.

Rate of Leading Neutron Production

Using the LEPTO Monte Carlo simulation to correct for the acceptance of the FNC, the fraction of DIS events with a neutron with $E_n \geq 100$ GeV is measured to be $(36^{+14}_{-9})\%$. This value is determined by correcting the fraction of observed events ($(2.6 \pm 0.4)\%$) for the FNC acceptance and resolution ($(7.8 \pm 2.0)\%$), and for the neutron detection efficiency of the calorimeter ($(93 \pm 5)\%$). The acceptance of the FNC depends upon the apertures of the beam line magnets and its effect on the observed energy spectrum is shown in Fig. 4A. The detection efficiency is less than 100% because of accidental coincidences in our veto hodoscopes which mostly originate from the back-scattering of charged particles produced during the neutron's hadronic shower. This inefficiency was estimated by measuring the rate of signals in our hodoscope planes as a function of the radial distance away from the neutron impact position. The LEPTO Monte Carlo predicts that 36% of DIS events contain a neutron with $E_n \geq 100$ GeV which is in agreement with our result.

In the kinematic range $E_n \geq 400$ GeV and $|t| < 0.5$ GeV^2, the fraction of DIS events containing a leading neutron is measured to be $(7.8^{+3.0}_{-2.0})\%$. The main source of the systematic error is the uncertainty in the FNC acceptance and energy resolution. The value of the FNC acceptance has been determined using the LEPTO and POMPYT Monte Carlo models and is equal to $(23 \pm 5)\%$. The ZEUS Collaboration obtain a consistent result for the fraction of DIS events containing a leading neutron with $E_n \geq 400$ GeV and $|t| < 0.5$ GeV^2 equal to $(9.1^{+3.6}_{-5.7})\%$ [23].

Measurement of $\mathrm{d}\sigma(ep \to e'nX)/\mathrm{d}z$

Fig. 7 shows the differential cross section $\mathrm{d}\sigma(ep \to e'nX)/\mathrm{d}z$ for events with $5 \leq Q^2 \leq 100$ GeV^2, $0.05 \leq y \leq 0.7$ and $|t| \leq 0.5$ GeV^2. We have unfolded our observed neutron energy spectrum, correcting for the FNC acceptance and energy resolution, in order to measure the differential cross section. A Gaussian distribution with $\sigma = (0.25 \pm 0.05)E'_n$, where E'_n is the true neutron energy, was used in our unfolding procedure. The maximum contribution to the systematic error is the uncertainty in the FNC acceptance and energy resolution which is approximately 20% for the two bins between $0.4 < z < 0.8$. The error bars show the full statistical and systematic errors added in quadrature. The expectations of the LEPTO and POMPYT Monte Carlo models, which are shown in Figure 7, are consistent with our measurement.

Summary

The results presented in this paper show that pion exchange and soft color interaction Monte Carlo models both give a good general description of high energy neutrons. The fraction of DIS events which contain a neutron with $E_n \geq 400$ GeV and $|t| \leq 0.5$ GeV^2 is $(7.8^{+3.0}_{-2.0})$%. Using the LEPTO Monte Carlo to correct for the FNC acceptance, approximately 36% of DIS events contain a high energy neutron with $E_n \geq 100$ GeV. The differential cross section $\mathrm{d}\sigma(ep \to e'nX)/\mathrm{d}z$ for events with $z > 0.4$ and $|t| \leq 0.5$ GeV^2 has been measured and is consistent with the expectations of the LEPTO and POMPYT Monte Carlo models.

Acknowledgements

We are grateful to the HERA machine group whose outstanding efforts have made and continue to make this experiment possible. We thank the engineers and technicians for their work in constructing and now maintaining the H1 detector, our funding agencies for financial support, the DESY technical staff for continual assistance, and the DESY directorate for the hospitality which they extend to the non-DESY members of the collaboration.

References

[1] Preliminary results determined using the 1995 H1 neutron calorimeter are in the proceedings of the 28th International Conference on High Energy Physics, pa02-063, Warsaw, Poland, July 1996.

[2] J. D. Sullivan, Phys. Rev. **D5**, 1732 (1972).

[3] R. Zoller, Z. Phys. **C53**, 443 (1992).

[4] H. Holtmann *et al.*, Phys. Lett. **B338**, 363 (1994).

[5] B. Kopeliovich, B. Povh and I. Potashnikova, Z. Phys. **C73**, 125 (1996).

[6] G. Ingelman, A. Edin and J. Rathsman, Comp. Phys. Comm. **101**, 108 (1997).

[7] P. Bruni, A. Edin and G. Ingelman, "POMPYT version 2.6 – A Monte Carlo to Simulate Diffractive Hard Scattering Processes", unpublished program manual.

[8] T. Ericson *et al.*, CERN-preprint CERN-TH/95-158, (1995).

[9] R. Arndt *et al.* Phys. Rev. **C49**, 2729 (1994).

[10] R. Timmermans *et al.*, Phys. Rev. Lett. **67**, 1074 (1991).

[11] R. Arndt *et al.* Phys. Rev. Lett. **65**, 157 (1990).

[12] R. Klomp *et al.*, Phys. Rev. **C44**, 1258 (1990).

[13] R. Koch and E. Pietarinen, Nucl. Phys. **A336**, 331 (1980).

[14] H. Holtmann *et al.*, Nucl. Phys. **A596**, 631 (1996).

[15] W. Koepf *et al.*, Phys. Rev. **D53**, 2586 (1995).

[16] M. Przybycien, A. Szczurek and G. Ingelman, Z. Phys. **C74**, 509 (1997).

[17] T. Sjöstrand, Comp. Phys. Comm. **39**, 347 (1986).

[18] A. Edin, G. Ingelman and J. Rathsman, "Quarkonium Production at the Tevatron through Soft Colour Interactions", hep-ph/9705311, 1997.

[19] D. Acosta *et al.*, Nucl. Instr. and Meth. **A294**, 193 (1990).

[20] T. Nunnemann, Diplomarbeit im Studiengang Physik,"Aufbau und Test eines Kleinwinkel–Neutronen–Kalorimeters für das Experiment H1", Universität Heidelberg, 1996.

[21] J. Botts *et al.*, Phys. Lett. **B304**, 159 (1993).

[22] M. Glück, E. Reya and A. Vogt, Z. Phys. **C53**, 651 (1992).

[23] M. Derrick *et al.*, ZEUS Collaboration, Phys. Lett. **B384**, 388 (1996).

Figures

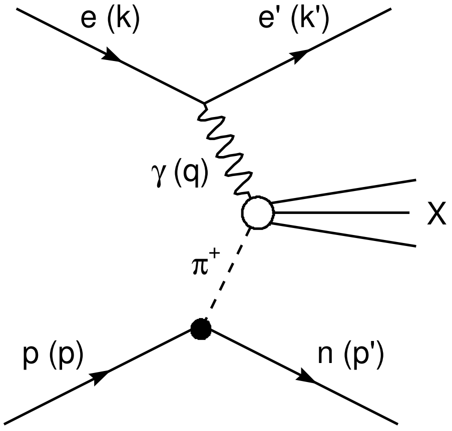

Figure 1: The pion exchange contribution to deep inelastic scattering.

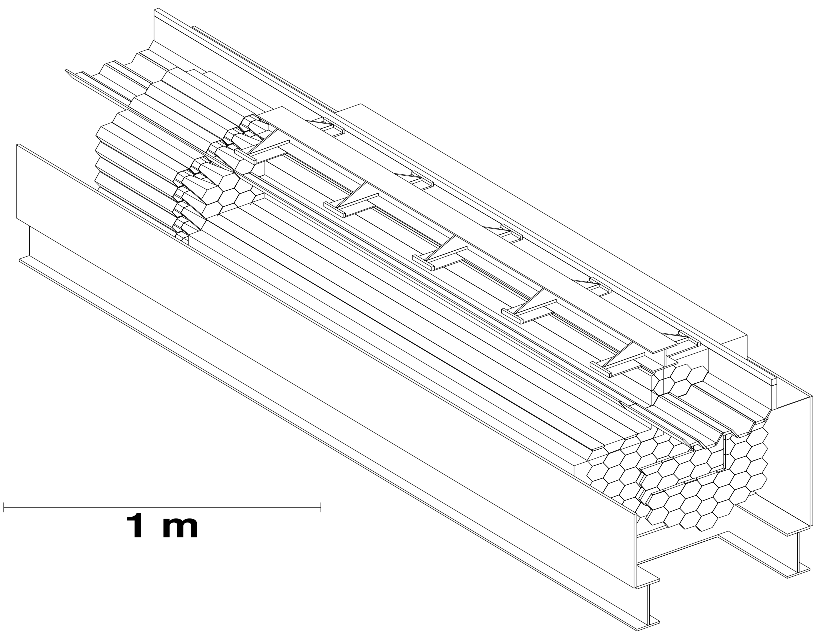

Figure 2: Configuration of the H1 forward neutron calorimeter.

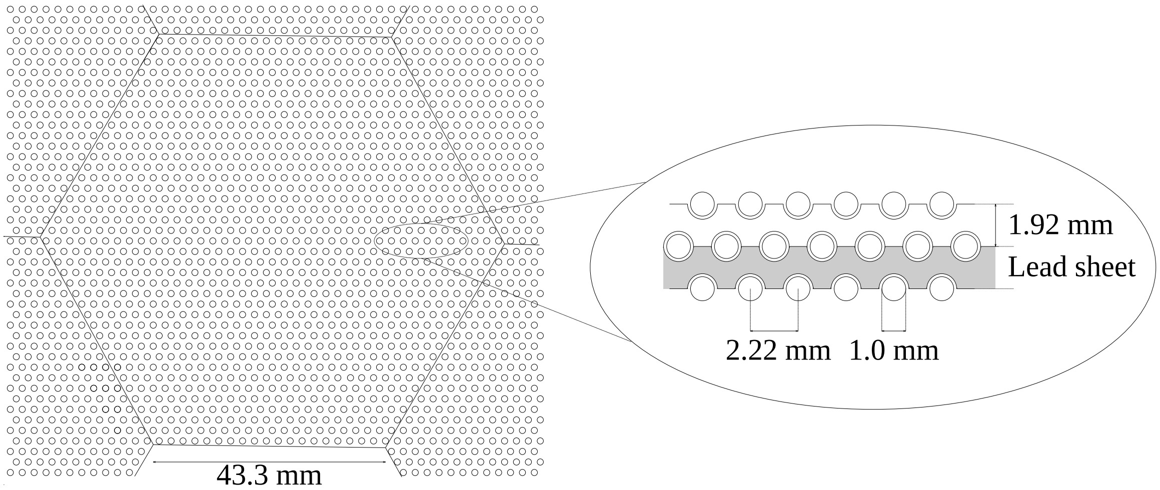

Figure 3: A detailed view of the lead/scintillating fiber matrix. The hexagonal structure is obtained by coupling 1141 scintillating fibers to a common photomultiplier located at the real of the calorimeter.

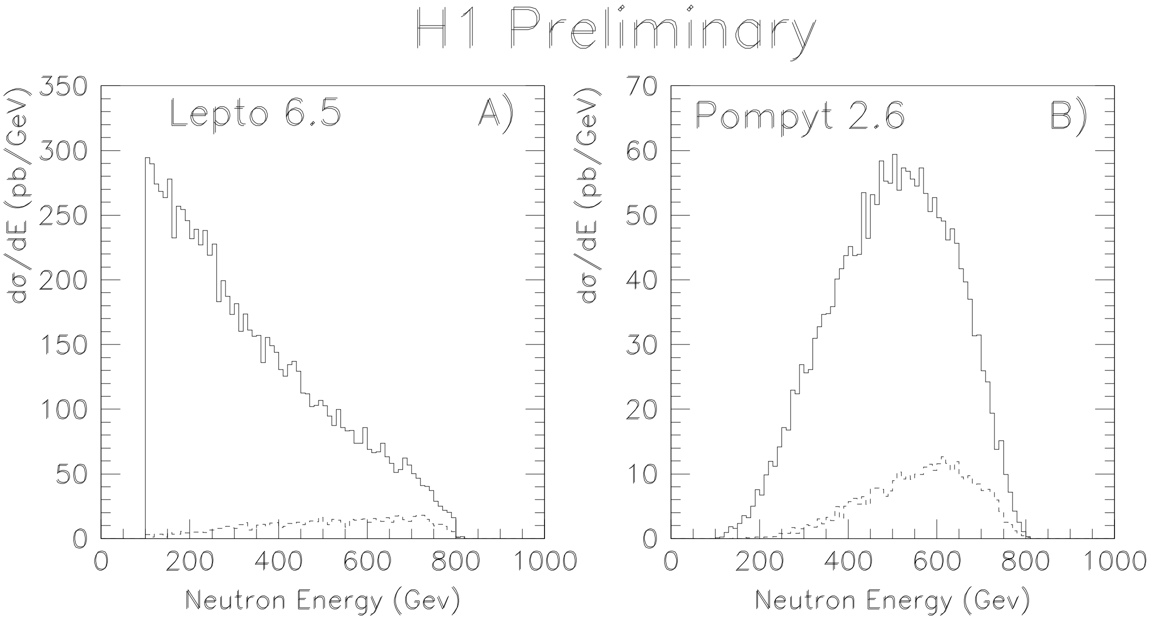

Figure 4: The solid curves show the generator level predictions from the LEPTO and POMPYT Monte Carlo programs for the energy spectra of neutrons with $E_n > 100$ GeV. The dashed curves show the predictions after the FNC acceptance has been taken into account. The CTEQ2L leading order parton distributions for the proton were used to calculate the LEPTO Monte Carlo predictions. The POMPYT Monte Carlo predictions were calculated using the GRV leading order parton distributions for the pion.

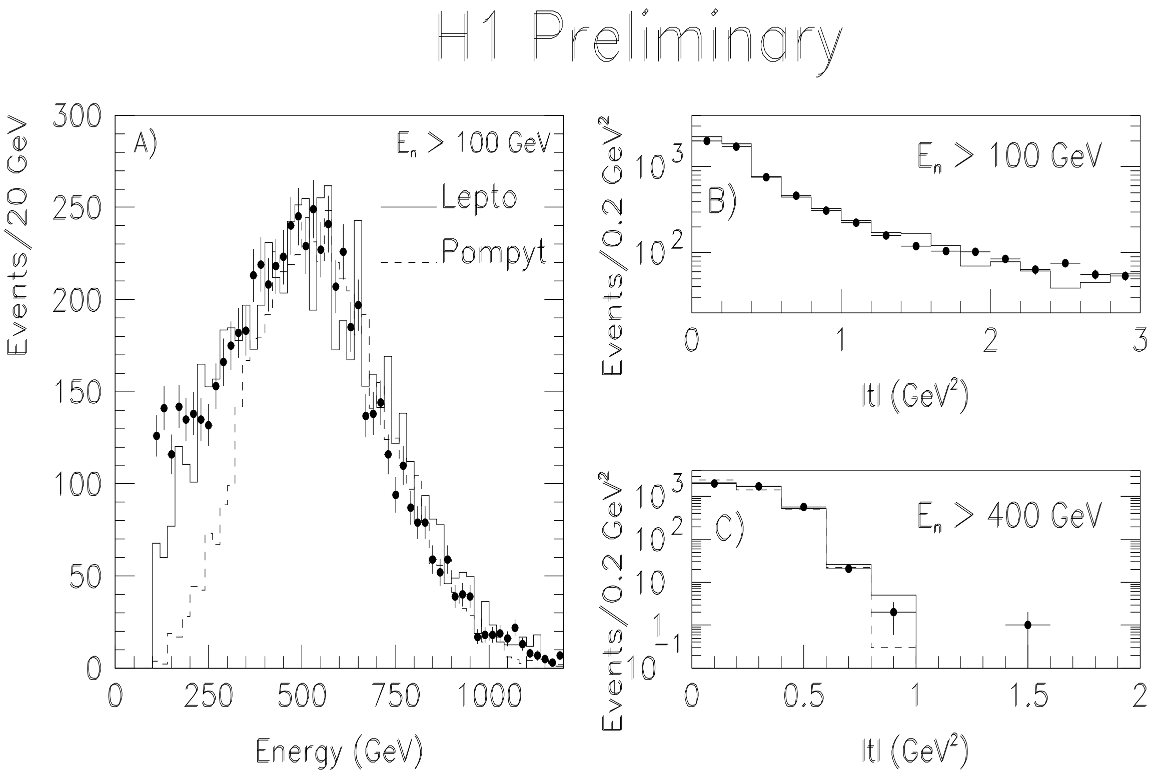

Figure 5: The observed neutron energy and $|t|$ distributions compared to the predictions of the LEPTO and POMPYT Monte Carlo models. The LEPTO Monte Carlo predictions are normalized to the number of events observed in the data with $E_n \geq 100$ GeV. The POMPYT predictions shown in A) and C) are normalized to the number of events observed in the data with $E_n \geq 400$ GeV.

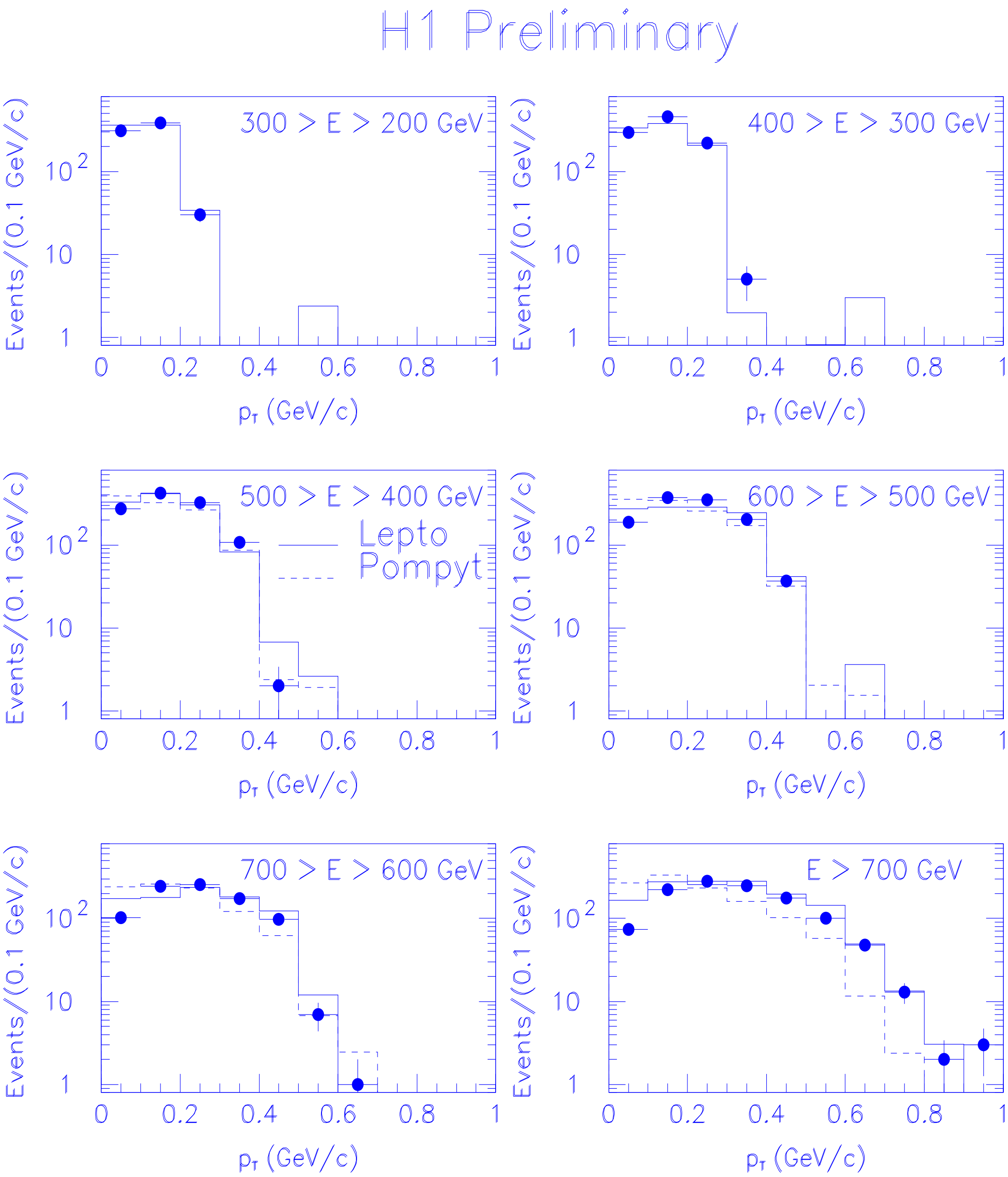

Figure 6: The observed p_T distributions in different energy ranges. The histograms show the predictions of the LEPTO and POMPYT Monte Carlo models after simulating the FNC acceptance and energy resolution. The LEPTO Monte Carlo predictions (solid histograms) are normalized to the number of events observed in the data with $E_n \geq 100$ GeV. The POMPYT predictions (dashed histograms) are normalized to the number of events observed in the data with $E_n \geq 400$ GeV and are only shown in this kinematic region.

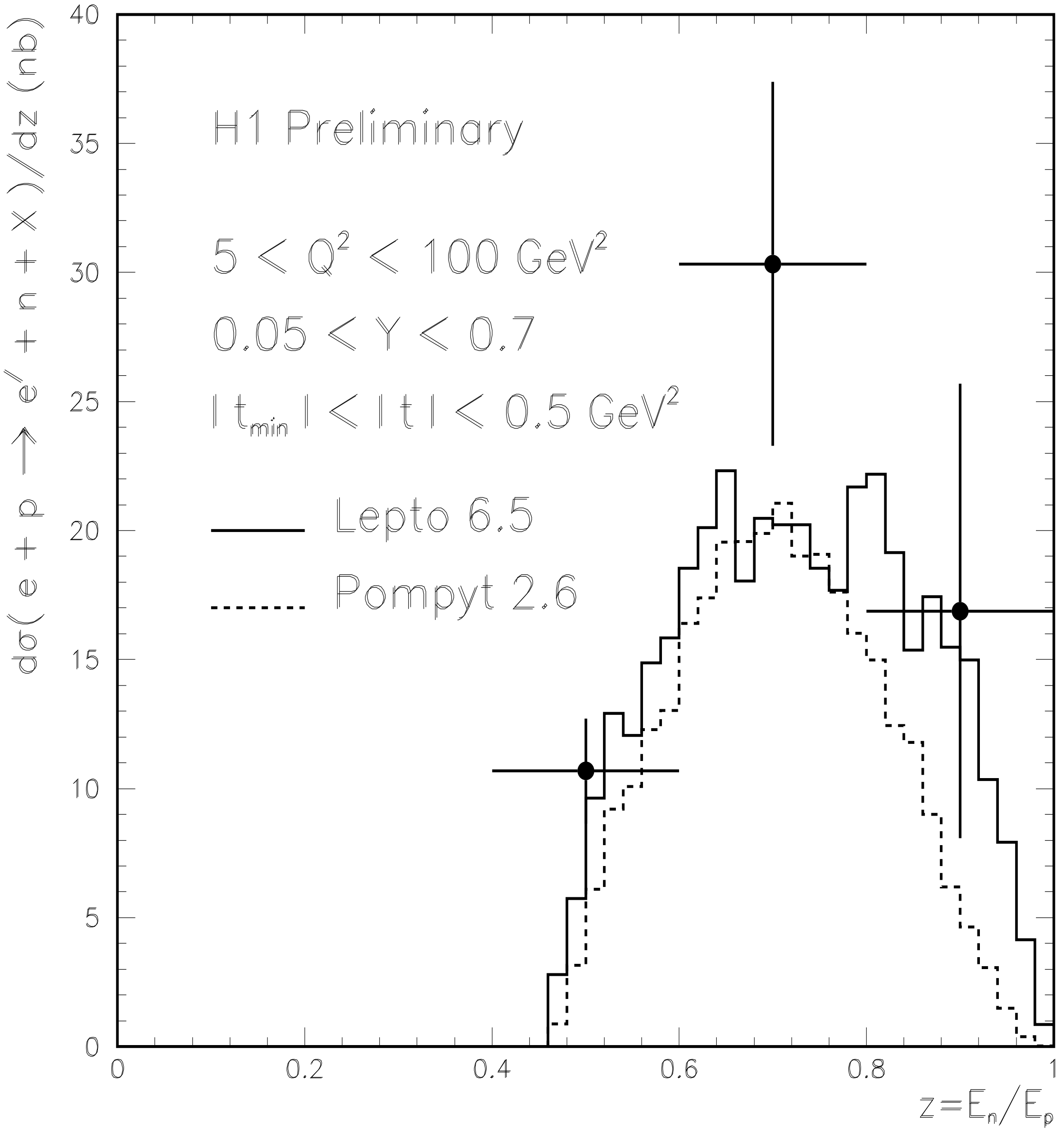

Figure 7: Measurement of $d\sigma(ep \to e'nX)/dz$ compared to the predictions of the LEPTO and POMPYT Monte Carlo models. The error bars show the full statistical and systematic error.